East Tennessee State University

Digital Commons @ East Tennessee State University

Electronic Theses and Dissertations

Student Works

5-2018

Kinetics and Activation Energy Parameters for Hydrolysis of Acetic Anhydride in a Water-Acetone Cosolvent System

Samson Olowoyo
East Tennessee State University

Follow this and additional works at: https://dc.etsu.edu/etd

Part of the Analytical Chemistry Commons

Recommended Citation

Kinetics and Activation Energy Parameters for Hydrolysis of Acetic Anhydride in a

Water-Acetone Cosolvent System

_____

A thesis

presented to

the faculty of the Department of Chemistry

East Tennessee State University

In partial fulfillment

of the requirements for the degree

Master of Science in Chemistry

_____

by

Samson Olanrewaju Olowoyo

May 2018

_____

Dr. Dane Scott, Chair

Dr. Gregory Bishop

Dr. Marina Roginskaya

Keywords: Eyring plot, activation parameters, hydrolysis, kinetics, acetic anhydride, cosolvent

systems

ABSTRACT

Kinetics and Activation Energy Parameters for Hydrolysis of Acetic Anhydride in a

Water-Acetone Cosolvent System

by

Samson Olanrewaju Olowoyo

The hydrolysis of acetic anhydride is a widely-studied liquid phase reaction studied since 1906.

Different approaches have been used to study the kinetics of this reaction. Approaches used by

researchers have involved the use of sophisticated experimental set-ups. In this work, the pH

technique has been adopted which involves the use of a pH meter to monitor the hydrolysis

reaction. Analysis of the hydrolysis reaction has been performed for water/acetone cosolvent

systems over a range of temperatures and mole fractions. Eyring analysis was performed under

isomole fraction conditions and activation enthalpy, entropy, and Gibbs free energy for

hydrolysis of acetic anhydride have been determined.

The isomole fraction Eyring plots are linear, because, activation enthalpy and entropy are

independent of temperature under these conditions. Activation free Gibbs energy increases with

increasing temperature at a constant water mole fraction, while it decreases with increasing water

mole fraction at constant temperature.

DEDICATION

This work is dedicated to Mr. and Mrs. Olowoyo, my brother-in-law Mr. Innocent Anetor, my brother Mr. Olusoji Olowoyo, my nephews (Jason Anetor and Ifeoluwa Sangodeyi) and my friends Kiyontre White, Emmanuel Ogunkunle, Ganiu Moshood, Nathan Mitchell, Ovuokenye Omadoko, Dimeji Shittu, and Munene Mwirigi.

ACKNOWLEDGEMENTS

To God the Almighty be the glory and praises for seeing me to the end of this work; which could not have been possible, if not for his grace. I wish to express my heartfelt gratitude and profound appreciation to everyone who has been extremely helpful to me in accomplishing this research.

I want to express my sincerest and warmest gratitude to my advisor, Dr. Dane Scott for his encouragement and supporting me during this research work. My heartfelt gratitude also goes to Dr. Marina Roginskaya and Dr. Gregory Bishop for their willingness to serve on my thesis advisory committee.

Also, to my mentor, my mother, and my sisters (Esther, Atinuke, Temitope) for being supportive and for their encouragement. I must confess you are my strength. May God bless you all. My profound gratitude to my Dad for being understanding and for his advice; I owe you my respect. Once again, my appreciation goes out to my Mom, who with her help and love I'm where I am today. I also want to thank Dr. Helen Alabi for her encouragement and guidance, I say a big thank you Ma!

TABLE OF CONTENTS

LIST OF TABLES

LIST OF FIGURES

LIST OF REACTION SCHEMES

LIST OF ABBREVIATIONS

k_{obs}	Observed reaction rate constant
K	Second order Eyring rate constant
K	Equilibrium constant
X_w	Water mole fraction
X	Mole fraction
‡	Transition state symbol
$\Delta S^{\ddagger}$	Activation entropy
$\Delta H^{\ddagger}$	Activation enthalpy
$\Delta G^{\ddagger}$	Activation Gibbs free energy
Uv-vis	Ultraviolet-visible
n.r.	Not Reported
H^+	Hydronium ion
k_B	Boltzmann's constant
R	Gas constant
H	Planck's constant
Y	$R\left\{\ln\left(\frac{hk_{obs}}{k_B T}\right) - \ln\left([H_2O]\right)\right\}$

CHAPTER 1

INTRODUCTION

Background Study

The understanding of the kinetics of a reaction allows us to predict the reaction rate. If the kinetics of a reaction is not fully understood, complications could arise leading to explosion of reaction mixture, damage to apparatus and equipment, and inadequate control over the reaction may occur.[1-2]

The hydrolysis of acetic anhydride is a fast exothermic reaction. The product, acetic acid, is a very important chemical compound.[1] Scientists have studied the hydrolysis of acetic anhydride with a variety of methods for measuring the rate of this reaction. Some of the advanced methods used over the years for the experiment include the use of UV-vis spectrophotometry with isoperibolic calorimetry. This reaction depends on the color change observed by the UV-vis spectrophotometry using an acid-base indicator.[3]

Haji and Erkey used an in-situ Fourier Transform Infrared Spectrophotometer (FTIR)[4], while Kralj measured the conductivity of acetic acid which is formed during the hydrolysis of acetic anhydride to study the reaction rate.[5] Hirota et al. studied hydrolysis of acetic anhydride by monitoring the calorimetric properties of the reaction in an adiabatic container.[2] Most of the techniques used for monitoring the rate of kinetics of hydrolysis of acetic anhydride revolve around colorimetric, calorimetric, volumetric, conductivity measurement and spectrophotometric analysis.[6]

The use of a co-solvent changes the rate of chemical reaction by orders of magnitude. The relationship between the solvent used in a reaction and the rate of reaction depends on the

interactions between the solvent, reacting species, and intermediates.[7] Below is a description of reagents and products carrying out hydrolysis of acetic anhydride.

Acetone

Acetone is a ketone with molecular formula $(CH_3)_2CO$. Acetone is a colorless, flammable, and volatile liquid. It serves as a good co-solvent in the present work because of its miscibility with water.[8]

Synthesis and Reactions of Acetic Anhydride

Dehydration of acetic acid gives acetic anhydride as shown in Scheme 1 below;
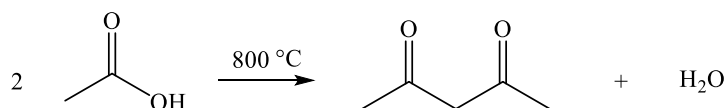
Scheme 1: Reaction of dehydration of acetic acid

Acetic anhydride is used for acetylation in numerous chemical reactions. The most prominent application is in the production of aspirin. There are many applications for industrial use and pharmaceutical uses.[9-10] Acetic anhydride is very reactive with water; its hydrolysis produces acetic acid. The reaction is explosive when conducted in strong acid such as H_2SO_4 and HNO_3.[10]

Acetic anhydride is a transparent liquid with a pungent-irritating smell. The liquid boils at 139 °C with a density of 1.080 g/mL at 15 °C. It is a flammable liquid slightly soluble in water (about 10% by mass) and reacts over time to give acetic acid.[9-11] Hirota made an observation about the reactivity of acetic anhydride: impurities are introduced into acetic anhydride due to constant opening of the reagent bottle and exposure to moisture in the air causing formation of

acetic acid.[2] Acetic anhydride is a biodegradable compound in the environment and undergoes photooxidative degradation in the atmosphere.

Acetic Acid

Acetic acid has been utilized by man since the middle ages.[10]
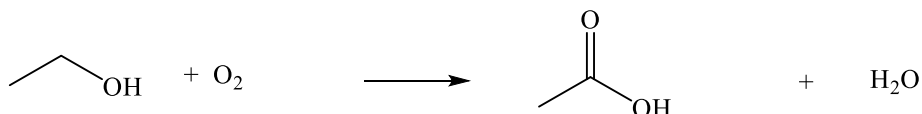
Scheme 2: Reaction of the production of acetic acid through fermentation[10]

Bacteria fermentation of ethanol produces acetic acid shown in Scheme 2. Acetic acid has a boiling point of $118\,°C$ and a density of 1.04 g/ml at $25\,°C$. The presence of hydrogen bonding in the molecule makes it highly soluble in different solutions.[10] Due to dissociation of acetic acid to give the hydronium ion, we can follow the hydrolysis of acetic anhydride reaction with a pH technique which is a measurement of the activity of the hydronium ion concentration.

Hydrolysis of Acetic Anhydride

The proper definition of hydrolysis as a chemical term would be the breaking and forming of chemical bonds by addition of water.[12] Hydrolysis is the exact opposite of condensation, in which a water molecule is lost from a reactant for the reaction to take place.[4] Scheme 3 shows the reaction of acetic anhydride forming acetic acid.
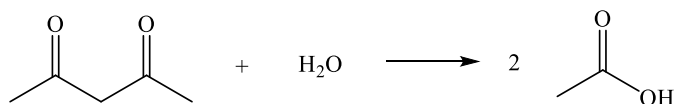
Scheme 3: Chemical equation of hydrolysis of acetic anhydride[13]

Possible Mechanism of Hydrolysis of Acetic Anhydride

The mechanism of hydrolysis of acetic anhydride does not occur through a classical substitution reaction, as observed with other carboxylic acid derivatives.[13] The mechanism occurs through three steps shown below in Scheme 4. The first step is addition of water, which is rate determining, followed by elimination and proton transfer to the liberated acetate resulting in two molecules of acetic acid. Computational work still in progress by collaborators Wiseman and Tamine indicate that only one water molecule is involved in the transition state.[14]
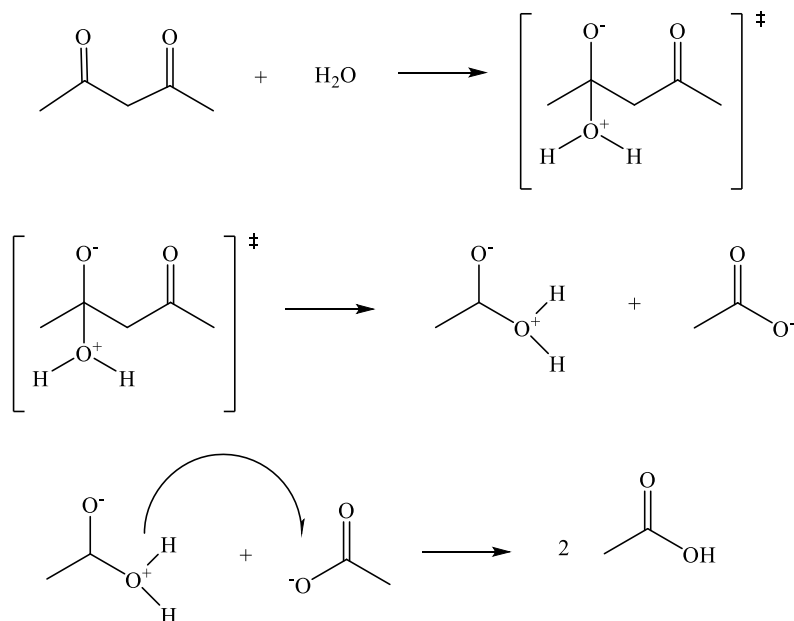
Scheme 4: Mechanism involved in the hydrolysis of acetic anhydride[2]

Transition-State Theory

Transition state theory was developed by Henry Eyring in the 1930's for calculation of the rate constant for a reaction. This transition state model involves the collision of the reactants to form an unstable intermediate.[15] Reactants (A and B) encounter an energy barrier which is the

minimum amount of energy needed for the reaction to take place. Once the reactants attain the energy called a "threshold energy", the reaction proceeds resulting in product.[16]

This theory is useful for determination of the rate of chemical reactions and aids in the calculation of activation enthalpy, entropy and Gibbs free energy if the reaction rate constant of the reaction is determined experimentally.[15-16] The key features of the transition state theory are that the activated complex is in a "quasi-equilibrium" state with the reactant species and that the rate of reaction can be calculated from the parameters of an activated complex, which is positioned on top of the peak of the potential energy curve.[17]
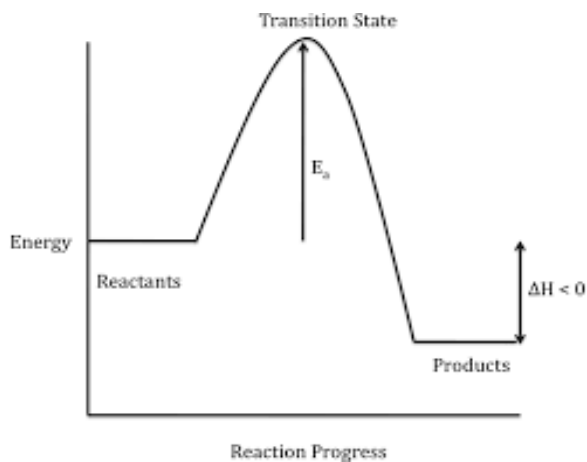
Figure 1: Energy profile diagram[16]

Figure 1 shows the energy diagram for an uncatalyzed exothermic reaction. The reaction is exothermic because the products possess less energy than the reactants, thereby releasing energy as the reaction occurs. The vertical line to the peak of the curve represents the activation energy. This theory is the basis of the Eyring rate equation. For a bimolecular reaction shown below, A and B are reactants, C is the product while $AB^{\ddagger}$ is the activated complex formed.[16]

$$A+B \longrightarrow C$$

$$A+B \underset{k_{-1}}{\overset{k_1}{\rightleftharpoons}} \left[AB^{\ddagger} \right] \xrightarrow{k_2} C$$
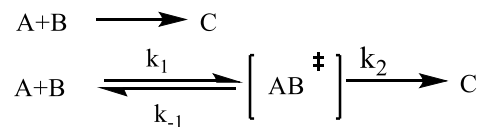
The reaction scheme above shows an equilibrium between reactants (A and B) and the transition-state complex. Eyring rate theory based on a transition-state complex was used in this work. Equation (1.1) shows the Eyring equation:

$$k = \frac{\kappa k_B T}{h} e^{-\frac{\Delta G^{\ddagger}}{RT}} \tag{1.1}$$

This work assumes that kappa (κ), transmission coefficient, is unity. This is because the transition state proceeds directly to the products without reverting back to the reactant species. All of $AB^{\ddagger}$ is assumed to form C.

$$\Delta G^{\ddagger} = \Delta H^{\ddagger} - T\Delta S^{\ddagger} \tag{1.2}$$

Substituting equation (1.2) for $\Delta G^{\ddagger}$ in equation (1.1) and taking the natural logarithm of both sides results in equation (1.3):

$$\ln\frac{k}{T} = \frac{-\Delta H^{\ddagger}}{RT} + \ln\frac{k_B}{h} + \frac{\Delta S^{\ddagger}}{R} \tag{1.3}$$
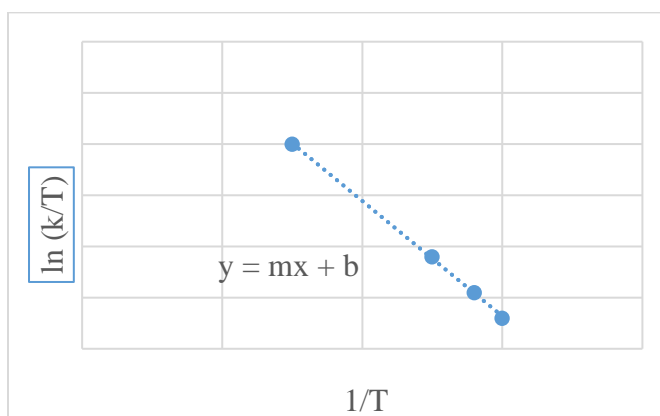
Figure 2: A theoretical Eyring plot

For the Eyring plot shown above, $\ln \frac{k}{T}$ vs. $\frac{1}{T}$ results in a straight line where the slope (m)

is $-\frac{\Delta H^{\ddagger}}{R}$ and intercept (b) is $\ln \frac{k_B}{h} + \frac{\Delta S^{\ddagger}}{R}$. Therefore, from the value of the slope and the

intercept, the activation enthalpy and entropy can be calculated. A modified version of the

Eyring equation was used in this work. The Eyring equation is rearranged below:

$$\ln \frac{k}{T} - \ln \frac{k_B}{h} = \frac{-\Delta H^{\ddagger}}{RT} + \frac{\Delta S^{\ddagger}}{R} \tag{1.4}$$

$$\ln \frac{kh}{k_B T} = \frac{\Delta S^{\ddagger}}{R} - \frac{\Delta H^{\ddagger}}{RT} \tag{1.5}$$

$$R \ln \left[\frac{kh}{k_B T}\right] = \Delta S^{\ddagger} - \frac{\Delta H^{\ddagger}}{RT} \tag{1.6}$$

The rate constant measured by the pH is a pseudo first-order rate constant called k_{obs}. The

reaction rate constant, k, is related to k_{obs} using equation (1.7) and (1.8) below:

$$k_{obs} = k[H_2O] \tag{1.7}$$

$$k = \frac{k_{obs}}{[H_2O]} \tag{1.8}$$

where k_{obs} is the experimentally observed rate constant and k is the second-order Eyring rate

constant.[14] The units of k and k_{obs} are $M^{-1}s^{-1}$ and s^{-1} respectively.

Substitution of equation (1.8) into (1.6) results in equation (1.9):

$$R \ln \frac{k_{obs} h}{[H_2O]k_B T} = \Delta S^{\ddagger} - \frac{-\Delta H^{\ddagger}}{T} \tag{1.9}$$

Separating the natural log of the water concentration results in:

$$R \left[\ln \frac{k_{obs} h}{k_B T} - \ln([H_2O])\right] = \Delta S^{\ddagger} - \frac{-\Delta H^{\ddagger}}{T} \tag{1.10}$$

17

Using Y for the left-hand side expression simplifies to equation (1.11):

$$Y = \Delta S^{\ddagger} - \frac{\Delta H^{\ddagger}}{T} \tag{1.11}$$

where $\Delta S^{\ddagger}$ is the activation entropy ($J \cdot mol^{-1} \cdot K^{-1}$) and $\Delta H^{\ddagger}$ is activation enthalpy ($kJ \cdot mol^{-1}$).

Plots of Y vs. $\frac{1}{T}$ were obtained where the slope and y-intercept permit calculation of the activation enthalpy, $\Delta H^{\ddagger}$, and entropy, $\Delta S^{\ddagger}$. Gibbs free energy of activation, $\Delta G^{\ddagger}$, was calculated using the Gibbs free energy equation where $\Delta G^{\ddagger} = \Delta H^{\ddagger} - T\Delta S^{\ddagger}$.

Just like the transition-state theory proposed by Eyring, the Arrhenius equation determines the temperature dependence on the rate of a chemical reaction.[18-19] The rate of a reaction depends on factors such as number of active collisions of the reactant species and activation energy.[15] The Arrhenius equation is shown below:

$$k = A \cdot e^{-\frac{E_a}{RT}} \tag{1.12}$$

$$\ln k = \ln A - \left(\frac{E_a}{RT}\right) \tag{1.13}$$

A plot of ln k against $\frac{1}{T}$ should result in straight line where the activation energy can be determined from the slope and pre-exponential factor calculated from the y-intercept.

<u>Thermodynamic Treatment of the Eyring Activation Parameters</u>

The variables measured in this work are temperature and co-solvent mole fraction.[14] Activation energy parameters of a chemical reaction are always determined with some level of uncertainty in experimental and theoretical calculations. The reaction rate parameters depend on several measurements resulting in systematic error.[20]

There are two different types of chemical kinetic measurements namely direct and indirect measurements. Direct chemical kinetic measurements involve the monitoring of the reaction conditions such that the measured parameters depend mainly on the activation rate parameters of a single reaction step. Indirect chemical kinetic measurements are also called bulk measurements. This mode of measurements depends on rate parameters of various step-wise reactions. The experimental results can be analyzed using a detailed reaction mechanism.[17]

Determination of the activation parameters of hydrolysis of acetic anhydride in this work is based on direct kinetic measurements.[17] The effect of temperature on the rate of reaction is best explained using the Arrhenius and Eyring equations provided previously. The Arrhenius reaction rate theory predicts that rate of chemical reaction increases with temperature while the Eyring equation is based on a transition-state model.[21]

Approaches to Studying Kinetics of Acetic Anhydride Hydrolysis

Scientists have used different techniques to study the kinetics of hydrolysis of acetic anhydride with methods such as colorimetry, titration, conductivity, spectroscopy and a combination of these techniques.[6] Haji and Erkey studied kinetics of hydrolysis of acetic anhydride by in-situ FTIR spectrophotometry.[4] The experiment was carried out in a batch reactor using three different temperatures. Shatynski and Haneisan studied a temperature vs. time dependence under adiabatic reaction conditions also using a batch reactor setup.[22] Temperature vs. time dependence was studied by other researchers such as Hirota et al., Shatnyski et al., and Glasser et al.[2-22-23] The temperature of the reaction was used to monitor the reaction progress and kinetic parameters were obtained by regression analysis.

Gold et al. used conductometric techniques for following the hydrolysis of acetic anhydride reaction. The effect of the solvent type and temperature on the kinetics of hydrolysis of acetic anhydride was explored.[24] Table 1 below is a summary of technique and literature values for the rate of hydrolysis of Acetic anhydride.

Table 1: Kinetic parameters for hydrolysis of acetic anhydride reported in the literature[2]

Reference	Techniques Used for Measurement	Activation Energy (kJ/mol)	ln k_{obs}	Unit of k_{obs}
King and Glasser (1965)	Calorimetry	39.8	9.93	s^{-1}
Eldridge and Piret (1950)	Titration	43.2	7.53	$M^{-1}s^{-1}$
Cleland and Wilhelm (1956)	Titration	44.4	7.80	s^{-1}
Bisio and Kabel (1985)	Calorimetry	46.5	12.80	s^{-1}
Glasser and Williams (1971)	Calorimetry	45.3	7.95	$M^{-1}s^{-1}$
Takashima (1971)	n.r.	49.4	18.1	s^{-1}
Shatynski and Hanesian (1993)	Calorimetry	46.9	12.74	s^{-1}
Wilsdon and Sidgwick(1913)	Conductivity	50.6	18.52	s^{-1}
Kralj (2007)	Conductivity	50.1	14.21	s^{-1}
Haji and Erkey (2005)	FTIR	53.6	15.48	s^{-1}
Asprey (1996)	Conductivity	45.7	7.66	$M^{-1}s^{-1}$

Justification of the Study

Hydrolysis of acetic anhydride is a well studied standard reaction used to test novel and modified laboratory techniques. Hydrolysis of acetic anhydride in co-solvents systems is not fully understood. Co-solvents are known to reduce the permittivity of the solution which slows the reaction rate. As such, co-solvent systems allow kinetic control of hydrolysis reactions. With

the exception of the work by Wiseman,[14] there are no studies of the kinetics of hydrolysis of acetic anhydride in water/acetone co-solvent systems. This work studies the kinetics of this system.

The advantages of using pH to determine the rate of hydrolysis of acetic anhydride include are that the experimental setup is simple and inexpensive, ease of analyzing the data and not having to stop the reaction for data acquisition.

Objectives of the Research

The overall aim of this research was to accurately determine kinetics parameters of the hydrolysis of acetic anhydride using different mole fractions of acetone at 20.00, 25.00, 30.00, 35.00, 40.00, 45.00, and 50.00±(0.01) °C. In this work, dependence of the rate constant of the hydrolysis of acetic anhydride has been determined for varying mole fractions of acetone and water. Acetone was chosen because it is water soluble and permits changing the polarity of the solvent without interfering with the hydrolysis of acetic anhydride and is widely used as a solvent in chemical reactions.[7] Acetic anhydride was added to the reaction mixture with the temperature regulated by the circulator. A plot of pH vs. time was obtained. Data analysis results in the rate constant for the hydrolysis of acetic anhydride.

CHAPTER 2

EXPERIMENTAL

Calibration of pH Probes

The pH was monitored using two Vernier BG Thermo-Scientific pH meters. The pH electrodes were calibrated before every trial. Buffer solutions with a pH of 4.00 and 7.00 were used because the pH changes measured occur in this range. Due to frequent use of the pH electrode, the electrodes required treatment due to the pH readings drifting over a few days but not during the experiment. The pH probes were soaked in 0.1 M HCl overnight. A long-term storage solution was prepared by adding 10 g of solid KCl to 100 mL to buffer solution (pH = 4.00).

After the acid soak, the probes were rinsed and placed in 75 mL of long-term storage solution for 30 to 60 min. After rinsing the probes, they were used for measurements and placed in a vial with normal buffer storage solution (pH = 4.00).

Preparation of Cosolvent

Calculated masses of water and acetone were measured by mass and added to a three-neck round-bottom flask. The water/acetone co-solvent solution, 75.00 mL, was prepared with 18 MΩ pure water and acetone. As an example, preparing a mole fraction of water (X_w) of 0.75 or mole fraction of acetone ($X_{acetone}$) of 0.25, the molar volumes for water (18.015 g/mol, d = 1.000 g/mL) and acetone (58.08 g/mol, d = 0.7845 g/mL) was found by dividing molar mass by density giving 18.015 mL/mol and 74.034 mL/mol respectively.

A volume acetone to water ratio was found by multiplying the desired mole fraction of acetone (0.25) by the molar volume of acetone and dividing by the product of mole fraction of water (0.75) and molar volume of water. The ratio was found to be 1.3699. The required volume, 75 mL, was set equal to the amount of water required (x) plus the amount of water (x) times the volume acetone to water ratio. Solving for x resulted in 31.64 mL of water. This value was multiplied by the volume acetone to water ratio which resulted in 43.53 mL of acetone required. The volumes of water and acetone were changed to masses using density. Table 2 below shows the volume of water and acetone for each water mole fraction (X_w) mixture.

Table 2: Calculated volumes for acetone-water cosolvent

X_w	Mass of Acetone (g)	Mass of H_2O (g)
0.75	34.011	31.647
0.83	26.891	40.714
0.87	22.384	46.461
0.89	30.724	35.850
0.92	15.507	55.306
0.95	10.466	61.665

Experimental Setup and Reaction Initiation

The flask was clamped in place in a water bath containing 75 mL of the reaction mixture. Temperature was controlled using a Fisher Scientific Isotemp 4100 R20. This automated equipment maintained a constant temperature during the experiment. The solution was homogenized using a stir bar controlled by a Troemner model 700 submersible magnetic stirrer placed in the Isotemp circulator below the round bottom flask. The pH probes were secured using large hole stoppers. The reaction was started by adding 188 µL of acetic anhydride using a Thermo-Scientific Finn Pipette F1. The pH vs. time data was collected using two Vernier glass-

body pH electrodes. Regression analysis was performed using Vernier Logger Pro 3.10.1 software to obtain the observed reaction rate.

Rate constants were obtained for water mole fraction of 1, 0.95, 0.92, 0.87, 0.83, 0.79, 0.75 at 20.00, 25.00, 30.00, 35.00, 40.00, 45.00, and 50.00($\pm$0.01) $^{\circ}$C. Triplicate or more trials were performed at each mole fraction and temperature. The experimental setup is shown is Figure 3 and 4.

Figure 3: Pictorial view of the experimental setup

Figure 4: Picture showing the Fisherbrand Scientific Water bath 4100 R20

CHAPTER 3

RESULTS

The pH vs time plot shown below is for acetone/water system at 25.00°C and a water mole fraction of 0.75.
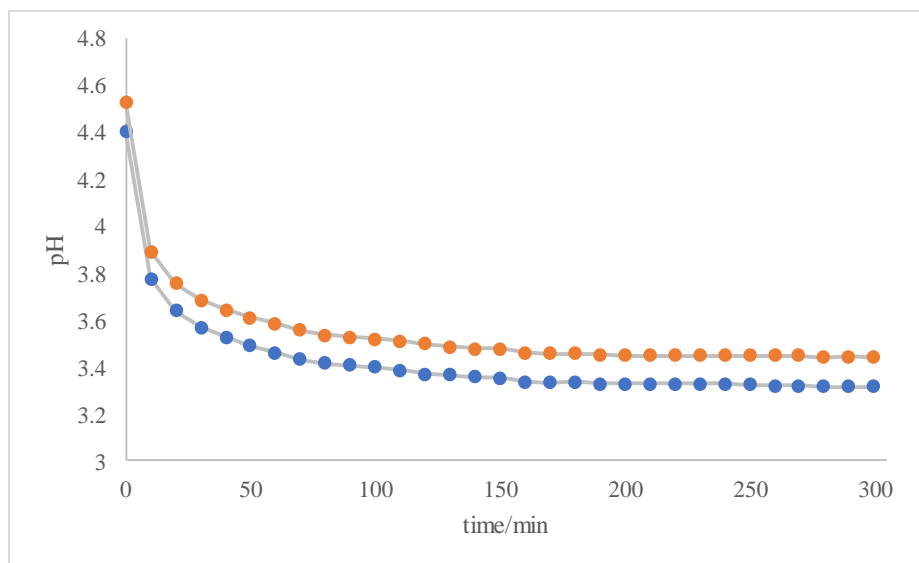
Figure 5: A plot of pH vs. time plot for the hydrolysis of acetic anhydride

Figure 5 above shows a pH vs. time plot for a water mole fraction of 0.75, where the orange and blue dots represent pH probe 1 and pH probe 2 readings respectively. Using plots similar to Figure 5 the observed rate constant was determined by fitting the data to a four parameter equation that relates pH to the observed rate constant. The ionization of acetic acid results in the hydronium ion and acetate ion which is why pH decreases with time. The equilibrium constant expression for the dissociation of acetic acid is shown below:

$$K_a = \frac{a_- a_+}{a} \tag{2.1}$$

where K_a is the equilibrium constant of acetic acid, a_-, a_+, a are the activities of acetate ion, hydronium ion and undissociated acetic acid respectively.

Through a series of assumptions and mass balance reactions, we arrive at equation (2.2) which is pH as a function of time for a non-buffered solution.

$$pH = -\log\frac{\gamma K_{acid}}{2\gamma_+} - \log\{\sqrt{1 + \frac{4\gamma_+^2[RCO_2H]_\infty}{\gamma K_{acid}}\left(1 - \frac{2[(RCO)_2O]_0 e^{-k_{obs}t}}{[RCO_2H]_\infty}\right)} - 1\} \qquad (2.2)$$

The pH vs time equation is simplified into four-parameters as shown in equation (2.3).

$$pH = a - \log\{\sqrt{1 + b(1 - ce^{-dt})} - 1\} \qquad (2.3)$$

In equation (2.3) a, b, c and d are called fitting parameters representing $-\log\frac{\gamma K_{acid}}{2\gamma_+}$, $\frac{4\gamma_+^2[RCO_2H]_\infty}{\gamma K_{acid}}$,

$\frac{2[(RCO)_2O]_0}{[RCO_2H]_\infty}$ and the observed rate constant in equation (2.2). Logger Pro software was used to

find k_{obs} by fitting equation (2.3).[6] Appendix A1 lists the observed rate constant data for

water/acetone co-solvent systems over a temperature range of 20.0-50.0 °C, where the mole

fraction of water ranged from 0.75-1.00.

Water concentrations in the appendix are from literature values or calculated.[14] As

triplicate trials or more were conducted, the average of the k_{obs} values, standard deviation,

percent error, and Y values are also reported. The k_{obs} values obtained for X_w of 1 (pure water

sample) are the fastest rates. The k_{obs} values increased with temperature at each mole fraction.

This trend is shown in Figure 6.
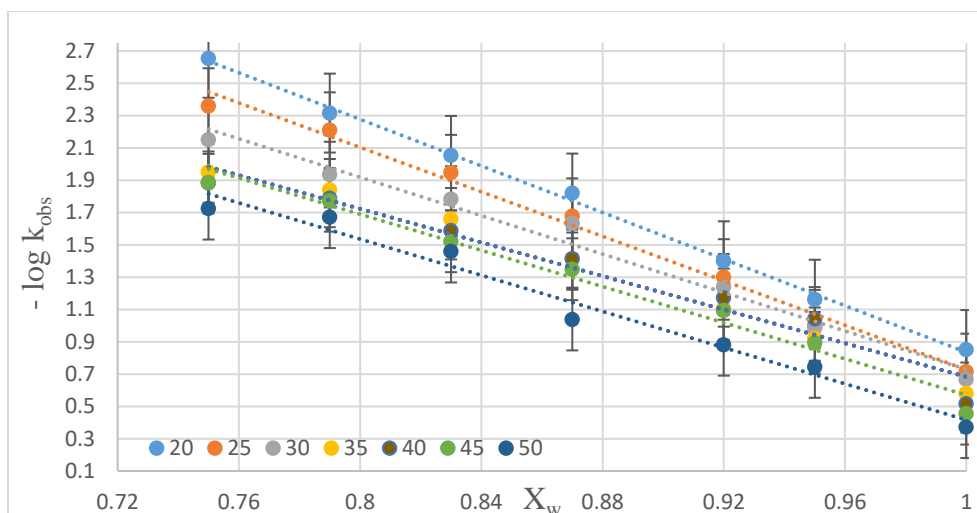
Figure 6: Plots of $-\log(k_{obs})$ vs. X_w for acetic anhydride hydrolysis in the acetone/water cosolvent system

The observed rate constants in Appendix A1 were used to generate isomole fraction Eyring plots in Figure 7. All data points are averages of at least triplicate measurements. The isomole fraction plots were analyzed using the expression; $Y = \Delta S^{\ddagger} - \frac{\Delta H^{\ddagger}}{T}$. These plots are linear meaning activation enthalpy and entropy are temperature independent at constant mole fractions of water.
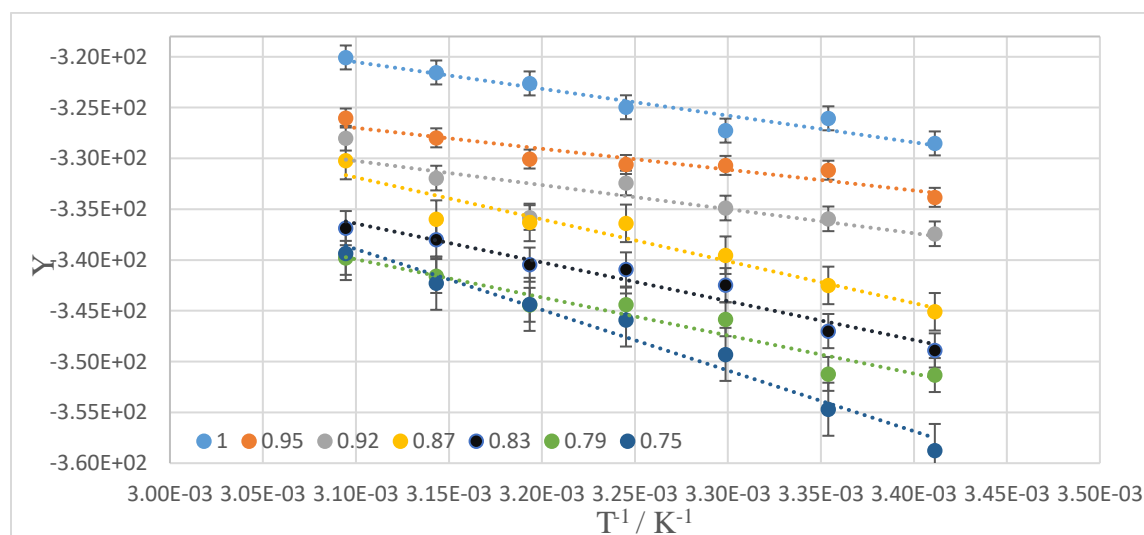
Figure 7: Iso-mole fraction Eyring plots for acetone/water cosolvent systems

In Figure 7, the temperatures from left to right are 50.00, 45.00, 40.00, 35.00, 30.00, 25.00, and 20.00($\pm$0.01) °C and mole fractions of water from top to bottom are 1, 0.95, 0.92, 0.87, 0.83, 0.79 and 0.75. Appendix A2 lists the activation enthalpy and entropy from the regression analyses using equation (1.11). These values were used to calculate activation Gibbs free energy through equation (1.2). Figure 8 shows that $\Delta G^{\ddagger}$ increases with temperature.
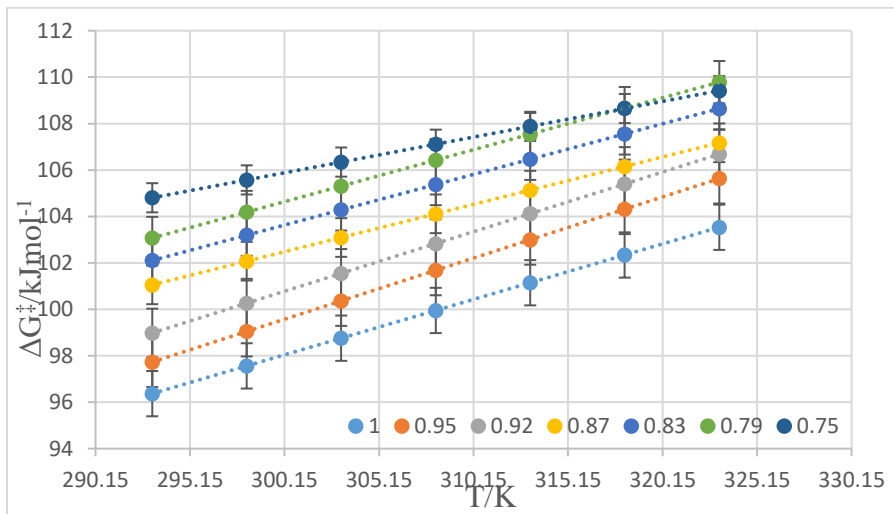
Figure 8: A plot of $\Delta G^{\ddagger}$ vs. T at constant X_w
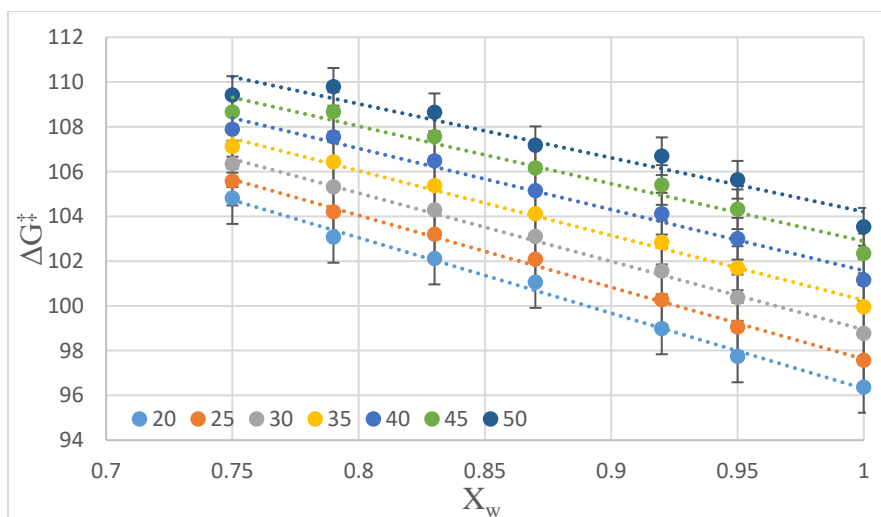
Figure 9: A plot of $\Delta G^{\ddagger}$ vs. X_w at constant T

Figure 9 shows a temperature range from 50.00 °C (top) to 20.00 °C (bottom), $\Delta G^{\ddagger}$ increases as mole fraction of water decreases and as temperature increases. Ideally, comparing the experimental reaction rate constants using acetone as a cosolvent to known values would be of value given the automated data acquisition method developed. This is the first report of observed reaction rates and activation energy parameters using acetone as a cosolvent and direct comparison is not possible. There are literature values using acetonitrile as a cosolvent for comparative purposes.[14] However, that data was collected using different mole fractions of water than in this work and some values were determined by extrapolation of experimental data. Comparison of values using mole fractions that differ by 0.01 is possible. Of interest are trends among the observed reaction rate and comparison of activation energy parameters.[14]

The negative logarithm of the observed rate constant at 25.00 °C and 50.00 °C at water mole fractions of 0.92 was 1.30 and 0.88 using acetone as a cosolvent. With acetonitrile at a mole fraction of water of 0.91 these values are reported as 1.35 and 0.65.[14] The values are nearly identical as water mole fraction water approaches pure water and become less using acetone compared to acetonitrile as water mole fraction decreases. While observed rates are nearly identical at low temperatures, rates at higher temperatures are faster using acetone as a cosolvent compared to acetonitrile. Using either cosolvent, the observed reaction rate increases with temperature and decreases as the mole fraction of water decreases.

For both acetonitrile and acetone cosolvent systems, the observed reaction rate was used to calculate the activation energy parameters by plotting Y vs. 1/T. Doing so permitted using the slope and intercept to find activation enthalpy and entropy ($\Delta H^{\ddagger}$ and $\Delta S^{\ddagger}$). The Y value is dependent on k_{obs}, T and [H_2O]. The Y values using acetonitrile or acetone as a cosolvent are nearly identical. Interestingly, all Y values are negative and increase with temperature at each

30

mole fraction of water. There are small deviations in the linearity of activation entropy and enthalpy values as temperature changes in the literature values using acetonitrile as a cosolvent. However, some activation enthalpy and activation entropy values were calculated by regression analysis because different mole fractions of water at each temperature were measured.[14]

There is a similar trend among activation energy parameters using acetone or acetonitrile as a cosolvent. The activation enthalpy ($\Delta H^{\ddagger}$) was found to range between 20 and 40 kJ/mol in this work which is identical to using acetonitrile ranging from 38-40 kJ/mol. Activation entropy ($\Delta S\ddagger$) in this work ranged from -204 to -273 J/K compared to -193 to -211 J/K using acetonitrile.[14] As in the case of using acetonitrile, when acetone is the cosolvent nearly 60% of the activation Gibbs free energy is due to activation entropy. As water mole fraction decreases, formation of the transition state complex is less favorable explaining why the observed reaction rate decreases.

Pure acetone has a permittivity of 20 while water is approximately 80.[25] When the cosolvent is added to generate a mole fraction of water of 0.83, the permittivity of the solution is approximately 56 compared to 65 for a solution of acetonitrile in which the water mole fraction is 65.[26] The dielectric constant of the cosolvent system has been shown to vary as water mole fraction decreases.[14] The trends and differences in activation energy parameters between using acetone and acetonitrile as a cosolvent are attributed to differences in permittivity the cosolvent in which the hydrolysis reaction is occurring.

CHAPTER 4

CONCLUSIONS

The importance of this study is determining the effect of the presence of acetone in water on the activation enthalpy ($\Delta H^{\ddagger}$), activation entropy ($\Delta S^{\ddagger}$) and activation Gibbs free energy ($\Delta G^{\ddagger}$). This is the first study determining these values for the hydrolysis of acetic anhydride using acetone as a cosolvent. A simple automated technique monitoring pH vs. time was developed to follow the hydrolysis reaction. The glass body pH probes were calibrated and treated periodically to prevent drift in measurements and pH data vs. time were collected. Temperature was controlled using a regulated water bath. The reaction was homogenized by using a submersible stirrer and magnetic bar.

The data was fit using a four parameter equation in which pH was determined as a function of time based on the dissociation of acetic acid, which is the main product of hydrolysis. In order to validate the system, the observed rate constant for hydrolysis of acetic anhydride was measured in pure water. The observed rate constant obtained at 35.00 °C was 0.23 min^{-1} which is identical within error compared to the value of 0.26 min^{-1} reported by Wiseman et al.[14] This served as validation that automated data collection was acceptable to carry out measurements of the observed reaction rate hydrolyzing acetic anhydride in water adding acetone as a cosolvent. The amount of acetone added was reported by using the value of water mole fraction. The observed rate of hydrolysis was measured at temperatures ranging from 20.00 to 50.00($\pm$0.01) °C.

The hydrolysis reaction of acetic anhydride in a water/acetone cosolvent systems forming acetic is pseudo-first order. The reaction mechanism begins by acetic anhydride reacting with

32

water, which results in a transition state complex. In literature, the number of water molecules that take part in forming the transition state is not certain. Regardless of the number of water molecules involved, the Eyring transition state theory used in this work assumes that once the transition state complex is formed the reaction progresses to form the products acetic acid and water. Both Eyring and Arrhenius rate theory predict that reaction rate increases with temperature. Values for the observed reaction rate agree with this trend. As mole fraction of water decreased, the observed reaction rate decreased.

Erying transition state theory does not account for the presence of cosolvent or change in dielectric constant of the solvent. Due to this, Eyring transition rate theory equations were modified to account for the change in water concentration as the mole fraction of water decreased. The observed reaction rate constant decreases with temperature as water mole fraction decreases. The Eyring equation was modified to use the observed rate to calculate activation energy parameters. This led to an analysis in which plots of Y vs. 1/T were obtained. Doing so permitted using the slope and intercept to find activation enthalpy and entropy ($\Delta H^{\ddagger}$ and $\Delta S^{\ddagger}$). These values were easily determined using LINEST arrays.

All Y values were found to be negative. The trend observed is that Y increases with temperature using each mole fraction of water. The Y values are dependent on k_{obs}, T and [H_2O]. The activation enthalpy and activation entropy are independent of temperature. In comparing activation energy parameters using acetone as a cosolvent to acetonitrile, these values were found to be similar at 25.00 °C. A majority of activation Gibbs free energy was determined to be due to activation entropy rather than enthalpy. This results in the transition state becoming less favorable as water mole fraction decreases causes the observed reaction rate to decrease. Differences between activation energy parameters using acetone as a cosolvent compared to

acetonitrile are attributed to the permittivity of the cosolvent systems at similar mole fractions of water.

Future Work

Similar work has been conducted on acetonitrile.[14] Other co-solvent systems such as tetrahydrofuran/water, dioxane/water, and alcohols/water will be explored. The purpose is to determine trends among different co-solvent systems. In addition, the effect of ionic strength on the reaction rate of hydrolysis reactions in co-solvent systems should be studied. Also, similar work can be performed on other anhydrides to uncover a trend in these hydrolyses reactions. Examples of other anhydrides include propanoic anhydride.

REFERENCES

1. Amenaghawon, NA; Osagie, EI; Osemwengie, SO. Modelling and simulation of the batch hydrolysis of acetic anhydride to produce acetic acid. *Nig. J. Tech.* (**2013**) 32:386-392.

2. Hirota, WH; Rodrigues, RB; Sayer, C; Guidi, R. Hydrolysis of acetic anhydride: Non-adiabatic calorimetric determination of kinetics and heat exchange. *Chem. Eng. Sci.* (**2010**) 65:3849–3858.

3. Ampelli, C; Di Bella, D; Lister, DG; Maschio, G; Parisi, J. The integration of an ultraviolet-visible spectrometer and a reaction calorimeter. *J. Th. Anal. Cal.* (**2003**) 72:875–883.

4. Haji, S; Erkey, C. Kinetics of hydrolysis of acetic anhydride by in-situ ftir spectroscopy. an experiment for the undergraduate laboratory. *Chem. Eng. Ed.* (**2005**) 39:56–61.

5. Kralj, AK. Checking the kinetics of acetic acid production by measuring the conductivity. *J. Ind. Eng. Chem.* (**2007**) 13:631-636.

6. Wiseman, FL. New insight on an old reaction – the aqueous hydrolysis of acetic anhydride. *J. Phy. Org. Chem.* (**2012**) 25:1105-1111.

7. Oakenfull, DG. The kinetics of the hydrolysis of acetic anhydride and the reaction of 4-nitrophenyl acetate with imidazole in aqueous-organic mixed solvents. *Aust. J. Chem.* (**1974**) 27:1423-31.

8. National center for biotechnology information. PubChem Compound Database: https://pubchem.ncbi.nlm.nih.gov/compound/acetone (accessed Mar. 27, 2018).

9. National center for biotechnology information. PubChem Compound Database:
    https://pubchem.ncbi.nlm.nih.gov/compound/acetic_anhydride (accessed Apr. 12, 2018).

10. Shakhashiri, BZ. General chemistry lecture note on acetic acid and acetic anhydride-
    chemical of the week. http://www.scifun.org/ (revised 30 Januray, 2008).

11. Caudri, JFM. The velocity of hydrolysis and alcoholysis of acetic anhydride in mixtures
    of water and ethyl or methyl alcohol. *J. F. Chem*. (**1929**) 547:292-951.

12. Lefers, M. Hydrolysis (updated July 26, 2004)
    http://groups.molbiosci.northwestern.edu/holmgren/Glossary/Definitions/Def-
    H/hydrolysis.html

13. Asprey, SP; Wojciechowski, BW; Rice, NM; Dorcas, A. Applications of temperature
    scanning in kinetic investigations: the hydrolysis of acetic anhydride. *Chem. Eng. Sci*.
    (**1996**) 51:4681-4692.

14. Wiseman, FL; Scott, DW; Cooper, WC; Tamine, J; O'Connella, R; Mitchell, N. Detailed
    thermodynamic analysis of the activation parameters for the simple hydrolysis of acetic
    anhydride in the acetonitrile/water cosolvent system. *RSC Adv*. (**2017**) 7:28965.

15. Pollak, E; Talkner, P. Reaction rate theory - what it was, where is it today, and where is it
    going? *Chaos.* (**2005**) 15:026116.

16. Keusch, P. Eyring equation. (retrieved May 2004)
    http://depa.fquim.unam.mx/amyd/archivero/Ecuacion_Eyring_7482.pdf

17. Tura´Nyi, T; Nagy, T; Gy. Zse´ Ly, I; Cserha´ Ti, M; Varga, T; Szabo´, BT; Kiss, PT;
    Zemple´Ni, A; Curran, HJ. Determination of rate parameters based on both direct and
    indirect measurements. *Intl J. of Chem. Kinetics*. (**2012**) 44:284-302.

18. Hindra, F; Oon-Doo, B. Kinetics of quality changes during food frying. *Critical Reviews in Food Science and Nutrition.* (**2006**) 46:239-58.

19. Laldler, JK; King, MC. The development of the transition state theory. *J. Phys. Chem.* (**1983**) 87:2657-2664.

20. Nagy, T; Turanyi, T. Uncertainty of Arrhenius parameters. *Intl. J. of Chem. Kinetics.* (**2011**) 43:359-378.

21. Eyring, H. The activated complex in chemical reactions. *J. Chem. Phys*. (**1935**) 3:107.

22. Shatynski, JJ; Hanesian, D. Adiabatic kinetic studies of the cytidine/acetic anhydride reaction by utilizing temperature versus time data. *Ind. Eng. Chem. Res.* (**1993**) 32:594-599.

23. Glasser, D; Williams, DF. The study of liquid phase kinetics using temperature as measured variable. *Ind. Eng. Chem. Fundam.* (**1971**) 10:516.

24. Gold, V. The hydrolysis of acetic anhydride. *J. Chem. Physics.* (**1947**) 44:506-518.

25. Maryott, AA; Smith, ER. Table of Dielectric Constants of Pure Liquids (Issued August 10, 1951) http://www.dtic.mil/dtic/tr/fulltext/u2/a278956.pdf

26. Scott, DW; Wiseman, FL; Cooper, WC; Alseiha, YS. Relative permittivity measurements of aqueous co-solvent systems including tetrahydrofuran. *J. Cdc.* (**2017**) 11:59-66.

SUPPLEMENTARY TABLES

Table A.1: Data for T^{-1}, k_{obs}, [H_2O] and Y values at given mole fraction of water. The error on all temperatures is ±0.01 °C.

X_w	T/K	T^{-1}/K^{-1}	k_{obs}/min^{-1}	[H_2O]/M	Y/J·mol·K
1	293.15	0.00341	0.141(±0.007)	55.405	328.53(±0.05)
	298.15	0.00335	0.192(±0.008)	55.337	326.06(±0.04)
	303.15	0.0033	0.17(±0.01)	55.254	-327.27(±0.06)
	308.15	0.00323	0.22(±0.02)	55.183	-324.97(±0.09)
	313.15	0.00319	0.30(±0.01)	55.016	-322.62(±0.03)
	318.15	0.00314	0.35(±0.01)	54.966	-321.54(±0.03)
	323.15	0.0031	0.42(±0.01)	54.843	-320.06(±0.02)
0.95	293.15	0.00341	0.069(±0.004)	51.191	-333.83(±0.06)
	298.15	0.00335	0.096(±0.004)	51.184	-331.16(±0.04)
	303.15	0.0033	0.103(±0.008)	51.040	-330.69(±0.08)
	308.15	0.00323	0.106(±0.004)	50.991	-330.60(±0.04)
	313.15	0.00319	0.114(±0.005)	50.797	-330.06(±0.04)
	318.15	0.00314	0.128(±0.007)	47.213	-327.98(±0.05)
	323.15	0.0031	0.18(±0.01)	47.586	-326.03(±0.06)
0.92	293.15	0.00341	0.041(±0.004)	47.280	-337.42(±0.10)
	298.15	0.00335	0.050(±0.004)	47.300	-335.95(±0.08)
	303.15	0.0033	0.058(±0.002)	47.113	-334.88(±0.03)
	308.15	0.00323	0.079(±0.006)	47.076	-332.42(±0.08)
	313.15	0.00319	0.053(±0.009)	46.863	-335.8(±0.2)
	318.15	0.00314	0.080(±0.008)	44.051	-331.9(±0.1)
	323.15	0.0031	0.13(±0.02)	44.07	-328.0(±0.2)
0.87	293.15	0.00341	0.0151(±0.0009)	43.67	-345.10(±0.06)
	298.15	0.00335	0.021(±0.002)	43.69	-342.5(±0.1)
	303.15	0.0033	0.0304(±0.0006)	43.47	-339.53(±0.02)
	308.15	0.00323	0.045(±0.005)	43.44	-336.4(±0.1)
	313.15	0.00319	0.046(±0.004)	43.21	-336.303(±0.09)
	318.15	0.00314	0.045(±0.006)	39.76	-336.0(±0.1)
	323.15	0.0031	0.09(±0.02)	40.06	-330.2(±0.2)

X_w	T/K	T^{-1}/K^{-1}	k_{obs}/min^{-1}	$[H_2O]/M$	Y/J/mol·K
0.83	293.15	0.00341	0.0883(±0.0005)	40.36	348.902(±0.006)
	298.15	0.00335	0.0113(±0.0006)	40.35	-347.00(±0.05)
	303.15	0.0033	0.020(±0.002)	40.12	-342.5(±0.1)
	308.15	0.00323	0.024(±0.003)	40.07	-340.9(±0.1)
	313.15	0.00319	0.0257(±0.0009)	39.85	-340.46(±0.04)
	318.15	0.00314	0.030(±0.006)	33.98	-339.3(±0.2)
	323.15	0.0031	0.035(±0.006)	33.84	-338.0(±0.2)
0.79	293.15	0.00341	0.0060(±0.0006)	36.61	-351.3(±0.1)
	298.15	0.00335	0.0062(±0.0005)	36.56	-351.21(±0.08)
	303.15	0.0033	0.012(±0.001)	36.28	-345.83(±0.08)
	308.15	0.00323	0.014(±0.001)	35.99	-344.38(±0.07)
	313.15	0.00319	0.014(±0.002)	36.00	-344.4(±0.1)
	318.15	0.00314	0.017(±0.002)	29.39	-341.580(±0.1)
	323.15	0.0031	0.0213(±0.0008)	29.46	-339.79(±0.04)
0.75	293.15	0.00341	0.0022(±0.0002)	33.45	-358.868(±0.09)
	298.15	0.00335	0.0037(±0.0003)	33.04	-358.749(±0.08)
	303.15	0.0033	0.0070(±0.0005)	33.00	354.69(±0.07)
	308.15	0.00323	0.011(±0.001)	32.69	-349.29(±0.09)
	313.15	0.00319	0.0130(±0.0004)	32.40	-345.907(±0.03)
	318.15	0.00314	0.0130(±0.0003)	32.41	-344.37(±0.02)
	323.15	0.0031	0.0188(±0.0005)	24.67	-342.29(±0.03)

Table A.2: Calculated values for activation energy, entropy, and Gibbs free energy for hydrolysis of acetic anhydride in acetone/water cosolvent systems. The error on all temperatures is ±0.01 °C.

X_w	T/K	$\Delta H^{\ddagger}/kJ.\,mol^{-1}$	$\Delta S^{\ddagger}/J.\,K^{-1}.\,mol^{-1}$	$\Delta G^{\ddagger}/kJ.\,mol^{-1}$
1	293.15	26.35(±3.32)	-238.85(±10.78)	96.37(±11.28)
	298.15	26.35(±3.32)	-238.85(±10.78)	97.56(±11.28)
	303.15	26.35(±3.32)	-238.85(±10.78)	98.76(±11.28)
	308.15	26.35(±3.32)	-238.85(±10.78)	99.95(±11.28)
	313.15	26.35(±3.32)	-238.85(±10.78)	101.15(±11.28)
	318.15	26.35(±3.32)	-238.85(±10.78)	102.34(±11.28)
	323.15	26.35(±3.32)	-238.85(±10.78)	103.53(±11.28)
0.95	293.15	20.52(±3.12)	-263.38(±10.29)	97.73(±10.75)
	298.15	20.52(±3.12)	-263.38(±10.29)	99.05(±10.75)
	303.15	20.52(±3.12)	-263.38(±10.29)	100.36(±10.75)
	308.15	20.52(±3.12)	-263.38(±10.29)	101.68(±10.75)
	313.15	20.52(±3.12)	-263.38(±10.29)	103.00(±10.75)
	318.15	20.52(±3.12)	-263.38(±10.29)	104.31(±10.75)
	323.15	20.52(±3.12)	-263.38(±10.29)	105.63(±10.75)
0.92	293.15	23.73(±6.78)	-256.70(±22.03)	98.98(±23.05)
	298.15	23.73(±6.78)	-256.70(±22.03)	100.27(±23.05)
	303.15	23.73(±6.78)	-256.70(±22.03)	101.55(±23.05)
	308.15	23.73(±6.78)	-256.70(±22.03)	102.83(±23.05)
	313.15	23.73(±6.78)	-256.70(±22.03)	104.12(±23.05)
	318.15	23.73(±6.78)	-256.70(±22.03)	105.40(±23.05)
	323.15	23.73(±6.78)	-256.70(±22.03)	106.68(±23.05)
0.87	293.15	41.26(±5.17)	-203.97(±16.79)	101.05(±17.57)
	298.15	41.26(±5.17)	-203.97(±16.79)	102.07(±17.57)
	303.15	41.26(±5.17)	-203.97(±16.79)	103.09(±17.57)
	308.15	41.26(±5.17)	-203.97(±16.79)	104.11(±17.57)
	313.15	41.26(±5.17)	-203.97(±16.79)	105.13(±17.57)
	318.15	41.26(±5.17)	-203.97(±16.79)	106.15(±17.57)
	323.15	41.26(±5.17)	-203.97(±16.79)	107.17(±17.57)

X_w	T/K	$\Delta H^{\ddagger}/kJ.\,mol^{-1}$	$\Delta S^{\ddagger}/J.\,K^{-1}.\,mol^{-1}$	$\Delta G^{\ddagger}/kJ.\,mol^{-1}$
0.83	293.15	38.17($\pm$3.64)	-218.09($\pm$11.85)	102.10($\pm$12.40)
	298.15	38.17($\pm$3.64)	-218.09($\pm$11.85)	103.19($\pm$12.40)
	303.15	38.17($\pm$3.64)	-218.09($\pm$11.85)	104.28($\pm$12.40)
	308.15	38.17($\pm$3.64)	-218.09($\pm$11.85)	105.37($\pm$12.40)
	313.15	38.17($\pm$3.64)	-218.09($\pm$11.85)	106.46($\pm$12.40)
	318.15	38.17($\pm$3.64)	-218.09($\pm$11.85)	107.56($\pm$12.40)
	323.15	38.17($\pm$3.64)	-218.09($\pm$11.85)	108.65($\pm$12.40)
0.79	293.15	37.49($\pm$4.39)	-223.71($\pm$14.26)	103.07($\pm$14.92)
	298.15	37.49($\pm$4.39)	-223.71($\pm$14.26)	104.19($\pm$14.92)
	303.15	37.49($\pm$4.39)	-223.71($\pm$14.26)	105.31($\pm$14.92)
	308.15	37.49($\pm$4.39)	-223.71($\pm$14.26)	106.43($\pm$14.92)
	313.15	37.49($\pm$4.39)	-223.71($\pm$14.26)	107.54($\pm$14.92)
	318.15	37.49($\pm$4.39)	-223.71($\pm$14.26)	108.66($\pm$14.92)
	323.15	37.49($\pm$4.39)	-223.71($\pm$14.26)	109.78($\pm$14.92)
0.75	293.15	59.73($\pm$4.59)	-153.76($\pm$14.92)	104.80($\pm$15.61)
	298.15	59.73($\pm$4.59)	-153.76($\pm$14.92)	105.57($\pm$15.61)
	303.15	59.73($\pm$4.59)	-153.76($\pm$14.92)	106.34($\pm$15.61)
	308.15	59.73($\pm$4.59)	-153.76($\pm$14.92)	107.11($\pm$15.61)
	313.15	59.73($\pm$4.59)	-153.76($\pm$14.92)	107.88($\pm$15.61)
	318.15	59.73($\pm$4.59)	-153.76($\pm$14.92)	108.65($\pm$15.61)
	323.15	59.73($\pm$4.59)	-153.76($\pm$14.92)	109.42($\pm$15.61)

VITA

SAMSON OLANREWAJU OLOWOYO

Education	B.S. Chemistry University of Ibadan,
	Ibadan, Oyo, Nigeria. (February, 2015)
	M.S. Chemistry East Tennessee State University,
	Johnson City, TN, USA. (May, 2018)
Professional Experience	Laboratory Intern, Glory Industries Limited,
	Ibadan, Nigeria. (April 2014 – June 2014)
	Support Chemist, Raw Materials Research and Development
	Council, Abuja, Nigeria. (May 2015 - June 2016)
	Graduate Teaching Assistant, East Tennessee State University
	Johnson City, TN, USA. (September 2015 - May 2018)
Honors/Awards	United States Opportunity Funds Scholarship - EducationUSA,
	United States Consulate, Abuja, Nigeria. (June 2015)
	Margaret Sells' Endowed Scholarship - East Tennessee State
	University, Johnson City, TN, USA. (October 2016)